International Journal of Heat and Fluid Flow 30 (2009) 691–699

Contents lists available at ScienceDirect

International Journal of Heat and Fluid Flow

journal homepage: www.elsevier.com/locate/ijhff

Effect of nanofluids on the performance of a miniature plate heat exchanger with modulated surface

M.N. Pantzali [a], A.G. Kanaris [a], K.D. Antoniadis [b], A.A. Mouza [a], S.V. Paras [a,*]

[a] Laboratory of Chemical Process and Plant Design, Department of Chemical Engineering, Aristotle University of Thessaloniki, Univ. Box 455, GR 54124 Thessaloniki, Greece
[b] Laboratory of Thermophysical Properties, Department of Chemical Engineering, Aristotle University of Thessaloniki, Univ. Box 453, GR 54124 Thessaloniki, Greece

ARTICLE INFO

Article history:
Received 11 September 2008
Received in revised form 17 December 2008
Accepted 13 February 2009
Available online 29 March 2009

Keywords:
Plate heat exchanger
Nanofluid
Thermophysical properties
CFD

ABSTRACT

In the present work, the effect of the use of a nanofluid in a miniature plate heat exchanger (PHE) with modulated surface has been studied both experimentally and numerically. First, the thermophysical properties (i.e., thermal conductivity, heat capacity, viscosity, density and surface tension) of a typical nanofluid (CuO in water, 4% v/v) were systematically measured. The effect of surface modulation on heat transfer augmentation and friction losses was then investigated by simulating the existing miniature PHE as well as a notional similar PHE with flat plate using a CFD code. Finally, the effect of the nanofluid on the PHE performance was studied and compared to that of a conventional cooling fluid (i.e., water). The results suggest that, for a given heat duty, the nanofluid volumetric flow rate required is lower than that of water causing lower pressure drop. As a result, smaller equipment and less pumping power are required. In conclusion, the use of the nanofluids seems to be a promising solution towards designing efficient heat exchanging systems, especially when the total volume of the equipment is the main issue. The only drawbacks so far are the high price and the possible instability of the nanoparticle suspensions.

1. Introduction

The need for efficient yet small in size heat transfer equipment has led to the development of compact plate heat exchangers (PHE) with modulated surface. Compared to a similar device with flat plates, the type of flow inside the PHE channels augments heat transfer due to flow separation and reattachment, whilst in the same time the complexity induced by the modulations significantly increases the friction losses (Kanaris et al., 2006). In an effort to develop more efficient heat exchanging systems, the research interest concerning the enhancement of the thermal capability of the working fluids has increased. In this frame, and although the application of suspensions of millimeter- or micrometer-sized particles in conventional liquids in order to enhance their thermal conductivity was proved unsuccessful, nanometer-sized solid particles are being considered the past few years. It seems that these suspensions, called *nanofluids*, exhibit an increased thermal conductivity compared to that of the base fluid, while, as the particles are ultra-fine and at low concentrations, they probably overcome the problems of sedimentation (Trisaksri and Wongwises, 2007).

The work done in the nanofluids area has been summarized in three recent reviews, i.e., Das et al. (2006), Trisaksri and Wongwises (2007) and Wang and Mujumdar (2007), where it is revealed that most of the recent work is mainly focused on the preparation methods and the study of the thermal conductivity of the suspensions. The evaluation of the use of nanofluids in heat exchanging equipment is an area where further investigation is needed (Das et al., 2006). The first experimental studies concerning convective heat transfer involve very simple flow configurations, such as laminar flows through straight tubes with a constant heat flux at the wall. For example, Wen and Ding (2004), Zeinali Heris et al. (2007) and Hwang et al. (2009) have investigated the use of Al_2O_3 nanofluids in horizontal tubes under laminar flow conditions and reported a significant heat transfer enhancement. Lee and Mudawar (2007) and Jung et al. (2009) have used similar nanofluids in laminar flow in microchannels, where a heat transfer enhancement is also detected. Pak and Cho (1998), Xuan and Li (2003) and Williams et al. (2008) have studied the application of various kinds of nanofluids in horizontal tubes under the turbulent regime. Pak and Cho (1998) and Xuan and Li (2003) have reported an increase in heat transfer rates. However, when the nanofluids are used and the results are compared in terms of liquid flow rates, the same authors, i.e., Pak and Cho (1998), report a decrease in heat transfer rates. Williams et al. (2008) observed no abnormal heat transfer enhancement and report that the usual correlations can predict the nanofluid performance, if accurate physical properties data are used. Mansour et al. (2007) used empirical correlations for heat transfer in a uniformly heated tube and reported that the advantages of utilizing nanofluids may vary significantly,

* Corresponding author. Tel.: +30 2310 996174.
E-mail address: paras@auth.gr (S.V. Paras).

0142-727X/$ - see front matter
doi:10.1016/j.ijheatfluidflow.2009.02.005

Nomenclature

A	plate heat exchanger area (m^2)
c_P	heat capacity (J/kg K)
F	LMTD correction factor (−)
k	thermal conductivity (W/m K)
L	characteristic length (m)
$LMTD$	log mean temperature difference (K)
m	mass-flow rate (kg/s)
Q	heat flow rate (W)
P	temperature efficiency (−), $P = (T_{co} - T_{ci})/(T_{hi} - T_{ci})$
R	heat capacity ratio (−), $R = (mc_P)_c/(mc_P)_h$
Re	Reynolds number (−)
T	temperature (K)
u	liquid velocity (m/s)
U	total heat transfer coefficient (W/m^2 K)
V	volumetric flow rate (m^3/s)

Greek letters

ΔP	pressure drop (Pa)
μ	dynamic viscosity (Pa s)
ρ	density (kg/m^3)
σ	surface tension (N/m)
φ	particle volume concentration (%)

Subscripts

c	cooling liquid
h	hot water
o	outlet
p	nanoparticles
t	theoretical
w	water

depending strongly not only on their thermophysical properties but also on the geometrical characteristics of the heat exchanging equipment and the operating conditions. Recently, Nguyen et al. (2007b), who studied the use of an aluminium oxide (Al_2O_3) nanofluid in an electronic liquid-cooling system, reported a considerable enhancement of the cooling convective heat transfer coefficient (up to 40%) for a particle volume concentration of about 7%.

Many numerical approaches have been attempted for the evaluation of the use of nanofluids in heat exchanging equipment. Since the solid particles are ultra-fine and easily fluidised, the most common method is to regard the nanofluid as a single-phase fluid, whose thermophysical properties are predicted by relevant theoretical models or correlations (Xuan and Roetzel, 2000). Studies using this approach, e.g. Tsai and Chein (2007) and Maiga et al. (2005), have proved that the addition of nanoparticles can significantly enhance the heat transfer rate. However, there is a lack of relevant experimental data that could be used to validate the calculated results.

In the present work, the effect of the use of nanofluid in a miniature PHE will be studied. A typical nanofluid will be selected and its thermophysical properties will be systematically measured. Next, the nanofluid will be applied in the miniature PHE and its performance will be compared to that of the base fluid (i.e., water). Numerical simulations will be conducted to study the effect of surface modulation on heat transfer augmentation and friction losses by simulating an existing miniature PHE and a notional similar PHE with flat plate. The CFD code will be also used to assess its reliability for applications with nanofluids and the results will be compared to the experimental data.

2. Selection of the nanofluid – measurement of its thermophysical properties

The thermophysical properties of various nanofluids containing mainly oxide nanoparticles (i.e., Al_2O_3, TiO_2 and CuO) have been studied in this Laboratory. Thermal conductivity measurements were carried out using the *transient hot-wire technique*. A detailed description of the method, along with an estimation of the uncertainty introduced, which in the case of nanofluids is better than 2%, is available elsewhere (Assael et al., 2004). The rheological behaviour was studied using a rheometer with coaxial cylinders (*Haake RheoStress RS600*) and the accuracy of the viscosity measurements is calculated to be about 5%. A differential scanning calorimeter (*SETARAM C80D*) was used for the measurement of the nanofluid specific heat capacity. The temperature of the sample and a reference substance is increased with the same rate and by measuring the difference in heat required, the specific heat of the sample is calculated with an accuracy estimated to be better than 3%. A surface tension meter employing the "pendant drop" method (*KSV® CAM 200*) was used for surface tension measurements with an accuracy better than 2%. The density is calculated by weighing a known volume of the nanofluid with an accuracy estimated at about 5%.

It was confirmed that both the stability of the suspensions and their thermophysical properties strongly depend on the volume fraction, the size, the shape and the type of the nanoparticles, as well as the physical properties of both the nanoparticles and the base fluid. During the aforementioned study, nanofluids containing copper oxide (CuO) nanoparticles gave the most promising results concerning thermal conductivity among other nanofluids tested. Therefore, a commercial nanofluid, containing 50% wt CuO nanoparticles with a mean particle diameter of 30 nm, was purchased from *Alfa Aesar®* and diluted by adding distilled water (*Carlo Erba Reagenti SpA, Water Plus for HPLC*) under mechanical stirring. The stability of the suspension at rest was satisfactory. A typical TEM image of a nanofluid sample is presented in Fig. 1. The thermophysical properties for three different concentrations (i.e., 8%, 4% and 2% particle volume concentration) were measured and are presented in Table 1, where the corresponding pure water properties are also included for comparison.

The study of the thermophysical properties confirmed the general trends reported in the literature (e.g. Wang and Mujumdar, 2007; Zhou and Ni, 2008) with respect to the base fluid, i.e.:

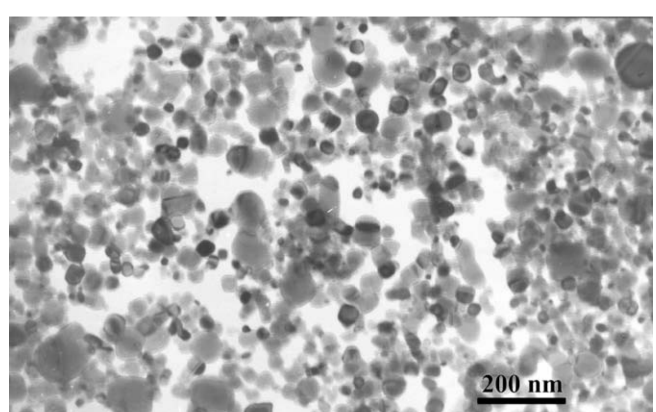

Fig. 1. Typical TEM image of the commercial copper oxide nanofluid.

Table 1
Measured thermophysical properties of the CuO nanofluids and water at 25 °C.

	Thermal conductivity (k_n, W/mK)	Heat capacity ($c_{P,n}$, J/kg K)	Viscosity (μ_n, mPa s)	Density (ρ_n, kg/m^3)	Surface tension (σ_n, mN/m)
CuO 8% v/v[a]	0.720	2700	5.6	1510	38
CuO 4% v/v	0.670	3280	2.0	1250	51
CuO 2% v/v	0.630	3720	1.3	1130	51
Water	0.607	4180	1.0	1000	72

[a] v/v: Particle volume fraction.

- The thermal conductivity increases.
- The density increases.
- The heat capacity decreases.
- The viscosity increases.

According to Williams et al. (2008), the advantages of using nanofluids depend on the relative increase of thermal conductivity and viscosity. The 2% particle volume fraction (v/v) suspension presents only a marginal increase in thermal conductivity (i.e., about 4%), while the viscosity of the 8% v/v suspension is too high (almost six times higher than water). Thus, a 4% particle volume concentration suspension is selected as a typical nanofluid for the heat transfer application, for which it is found that:

- The *thermal conductivity* increases about 10% with respect to water. This value is a little lower than the values measured by Das et al. (2003) and Lee et al. (1999) (about 14% and 12% increase compared to water, respectively) and it can be quite accurately predicted ($k_{n,t}$ = 0.679 W/m K) by the Hamilton–Crosser model (Das et al., 2006).
- The *density*, ρ_n, is almost 25% higher than that of pure water and can be well predicted by the classical two-phase mixture equation (Roy et al., 2004).
- The measured nanofluid *specific heat capacity*, $c_{P,n}$, is 20% lower than that of the base fluid and can be well predicted by Eq. (1) (Xuan and Roetzel, 2000). However, the equation proposed by Pak and Cho (1998), Eq. (2), overpredicts its value ($c_{P,n,t}$ = 4034 J/kg K), as also recently reported by Zhou and Ni (2008) for an Al_2O_3 nanofluid:

$$c_{P,n,t} = \frac{\varphi \rho_p c_{P,p} + (1-\varphi)\rho_w c_{P,w}}{\rho_n} \quad (1)$$

$$c_{P,n,t} = \varphi c_{P,p} + (1-\varphi) c_{P,w} \quad (2)$$

where φ is the particle volume fraction, ρ and c_P is the density and specific heat capacity, respectively of the nanoparticles (p) and water (w). The nanoparticle heat capacity, $c_{P,p}$, is taken equal to 530 J/kg K (Leitner et al., 2000).

- It exhibits practically Newtonian behaviour and the *viscosity* measured is significantly higher (almost 100%) than that of water, which is in agreement with the measurements of Nguyen et al. (2007a). The commonly used Einstein's equation (e.g. Lee and Mudawar, 2007), as well as its modifications, considerably underestimates the nanofluid viscosity ($\mu_{n,t}$ = 1.1 mPa s). The correlation by Nguyen et al. (2007a), proposed specifically for a 4% aqueous CuO nanofluid Eq. (3), gives a relatively accurate prediction (i.e., $\mu_{n,t}$ = 1.7 mPa s).

$$\mu_{n,t} = \mu_w (2.1275 - 0.0215 \cdot T + 0.0002 \cdot T^2) \quad (3)$$

where μ_w is the water viscosity and T the temperature in °C.

- The surface tension is lower than water, but this could be attributed to the possible addition of surfactants during the manufacturing procedure for the stabilization of the suspension.
- The product of density by heat capacity ($\rho_n \cdot c_{P,n}$) is practically equal to that of water.

3. Experimental setup

Since the commercial nanofluids are rather expensive, the heat exchanging experiments were conducted in a miniature PHE (Fig. 2a), which needs a small quantity of cooling liquid for its operation. This *PHE* is part of a commercial CPU liquid-cooling kit (*Gigabyte® 3D Galaxy, GH-WIU01*) and comprises a small copper plate having pin-fins placed on a corrugated pedestal on one of its sides. A plastic cover is firmly placed atop this plate, creating the flow path for the cooling liquid. The dimensions of the plate are 6 × 6 cm, while the modulated surface, where the heat transfer takes place, is circular with a diameter of 5.6 cm. The other side of the copper plate is flat and is placed in contact with a cell, also made of copper, where hot water flows. In order to minimise thermal contact resistance between the miniature PHE and the hot water cell, a thin film of high thermal conductivity grease has been applied. To eliminate heat losses the setup (Fig. 2b) is thermally insulated. The main heat exchanging unit is suitably adapted to the flow loop presented in Fig. 2c. The water passes through a heater and its temperature is controlled at about 55 °C. Its flow rate is adjusted using a high-accuracy valve and measured using an electro-optical flow meter (*McMillan, S-111*). The cooling liquid is stored in a half-litre container and is recirculated by means of a centrifugal pump. Before entering the PHE, the cooling liquid is cooled using a bath, so that the inlet temperature is set at a constant value, i.e., 14 °C. The flow rate of the cooling liquid is adjusted using a high-accuracy valve and in the case of water it is measured using another electro-optical flow meter (*McMillan, S-111*). As the aforementioned flow meter is suitable only for transparent liquids, in the case of the black-coloured CuO nanofluid the flow rate is measured using an online weighing system connected to a PC. The liquid flow measurements accuracy is estimated to be less than 4%.

Temperature data are acquired using high-accuracy T-type thermocouples (*Omega®*), located at the inlet and outlet of both streams. A T-type thermocouple is also placed between the two metal surfaces that are in contact. The thermocouples, whose accuracy has been estimated to be ±0.2 K, are connected through an A/D card (*Advantech®*, *PCI-1710HG*) to a PC for temperature monitoring and recording. The pressure drop between two taps located at the entrance and the exit of the cooling liquid conduit is measured using a differential pressure transducer (*Validyne®*, *DP103*) with an accuracy of 0.25% according to the manufacturer.

Prior to each experiment the flow rates of the two streams were adjusted and, after steady state was established, the data were recorded. After that, the cooling liquid flow rate was increased and new data were recorded. The above procedure was repeated for various hot water flow rates.

4. Computational procedure

As previously mentioned, a commercial *CFD* code (*ANSYS CFX® 10.0*), previously validated in this Laboratory (Kanaris et al., 2006), is employed:

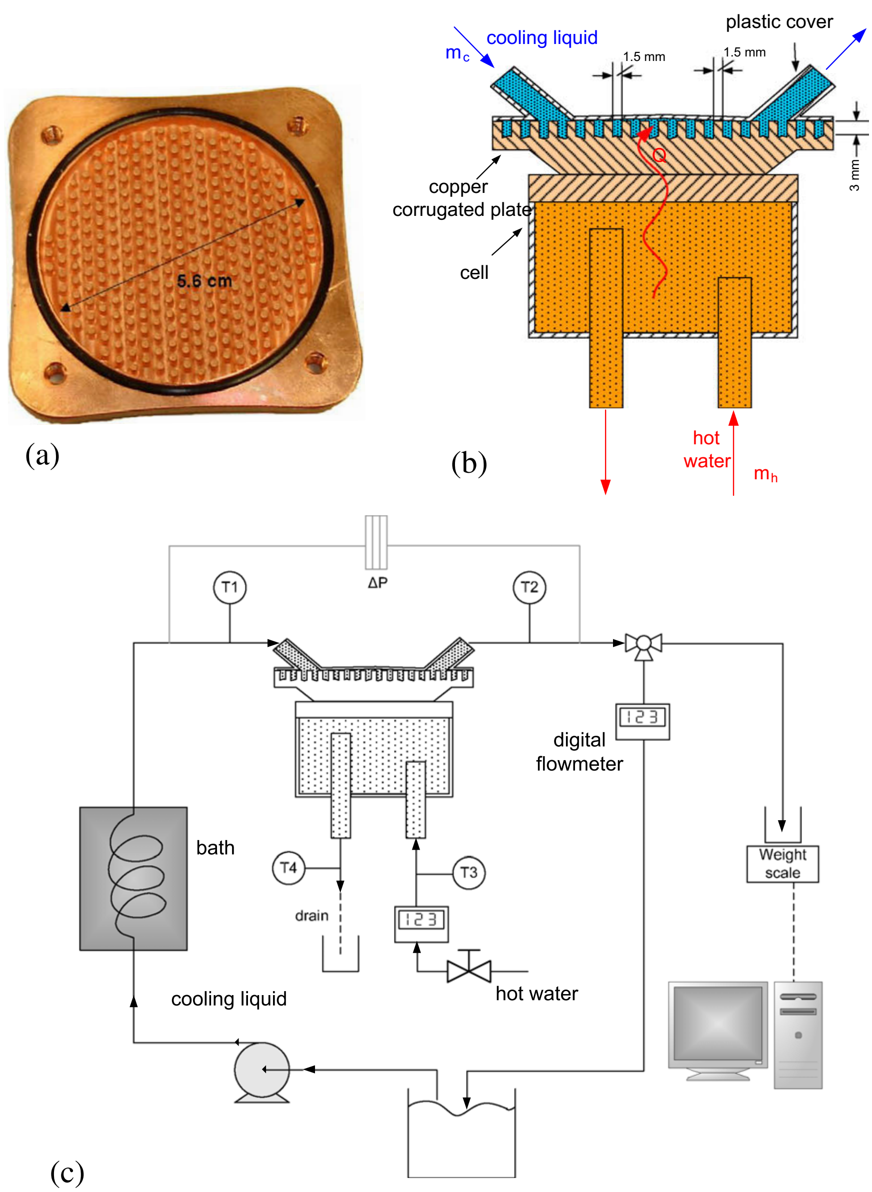

Fig. 2. (a) Photo of the PHE modulated copper plate, (b) schematic representation of the heat exchanging unit, and (c) flow loop.

- to study the effect of surface modulation on heat transfer augmentation and friction losses by simulating the miniature PHE and a notional similar PHE with flat plate; and
- to simulate the use of water and the nanofluid as cooling liquids and compare the results with the experimental data, in order to evaluate the reliability of such a code for nanofluid applications in this kind of equipment.

It is reported (Ciofalo et al., 1998; Hesselgraves, 2001; Kanaris et al., 2006) that, due to the high complexity of the conduit passages in PHEs, the flow is turbulent even for low Reynolds numbers, *Re*. Thus, the selection of the most appropriate turbulence model is an important step towards the simulation of a PHE channel. The most common two-equation turbulence model is k–ε, based on the equations for the turbulence energy, k, and its dissipation, ε. The k–ε model can successfully simulate highly turbulent flows but it has difficulties in simulating the flow near the surface. Menter and Esch (2001) report that the standard k–ε model overpredicts wall shear stress and heat flux, especially for the lower range of *Re* encountered in this kind of equipment.

An alternative to k–ε model is the k–ω model, developed by Wilcox (1988), which by using the turbulence frequency, ω, instead of ε, provides good simulation of the flow near the wall. Although this model is more robust and does not require very fine grid near the wall, it is sensitive to the bulk stream flow values of ω, outside the boundary layer. A combination of the two turbulence models, k–ε and k–ω, is performed by the SST (shear stress transport) model. This model activates the k–ω near the wall and switches to k–ε for the rest of the flow, thus using each model where it performs best. Previous work in this Lab concerning PHEs has proved that the SST model is the most appropriate for simulating the flow inside this type of conduit (Kanaris et al., 2006).

The computational model is designed in the parametric environment of *ANSYS Workbench*. It consists of separate computational domains for the fluid and the solid parts of the model. The grid used for the simulation is an unstructured mesh with tetrahedral elements. The quality of the grid as well as the effect of its density to the solution is probed (Table 2) and the final grid for the computational domain for the fluid inside the miniature PHE consists of approximately 1,660,000 elements, while the grid for the solid part

Table 2
Typical grid dependence study results ($Re = 100$).

Fluid domain elements (approximately)	Solid domain elements (approximately)	T_{co} (K)	Pressure drop (Pa)
850,000	1,160,000	294.7	261
1,420,000	1,260,000	291.3	242
1,660,000	1,310,000	291.0	236

of the miniature PHE consists of approximately 1,310,000 elements. Near the walls of the miniature PHE, where the k–ω model is activated, a layer of prismatic elements is imposed for $y^+ < 1$ to facilitate the boundary layer calculations. It is obvious that the elements are not distributed uniformly, but finer grid is focused near the solid walls of the PHE. The computational domain is presented in Fig. 3a, while a detail of the grid is presented in Fig. 3b.

The complexity of the channel geometry combined with the need for a fine grid near the wall and around the pin-fins lead to a high increase of computational demands. For the needs of the present study, a high performance parallel computing cluster (HPC), which consists of six 64-bit *AMD* processors and a total of 16 GB RAM, was employed. The *HPC* uses Gbit Ethernet connections and runs *Gentoo Linux*, while the commercial *CFD* code uses the *MPICH* protocol for messaging between the nodes.

Water and CuO nanofluid were used as working fluids for the simulation. The fluid thermophysical properties were changed accordingly in each case and the nanofluid was treated as a single-phase fluid, which is, as already reported, the most common approach. A pseudo-steady state simulation is performed, which uses a physical time-step for the computations (CFX Manual, 2005). Non-isothermal flow is considered for all simulations. A mass-flow and a pressure boundary condition were set on the entrance and on the exit of the PHE, respectively. A domain interface boundary condition is set between the fluid and the solid computational domains allowing the different grids to interchange data. Regarding the convergence, the high-resolution advection scheme was selected for the simulations and the double-precision solver was used.

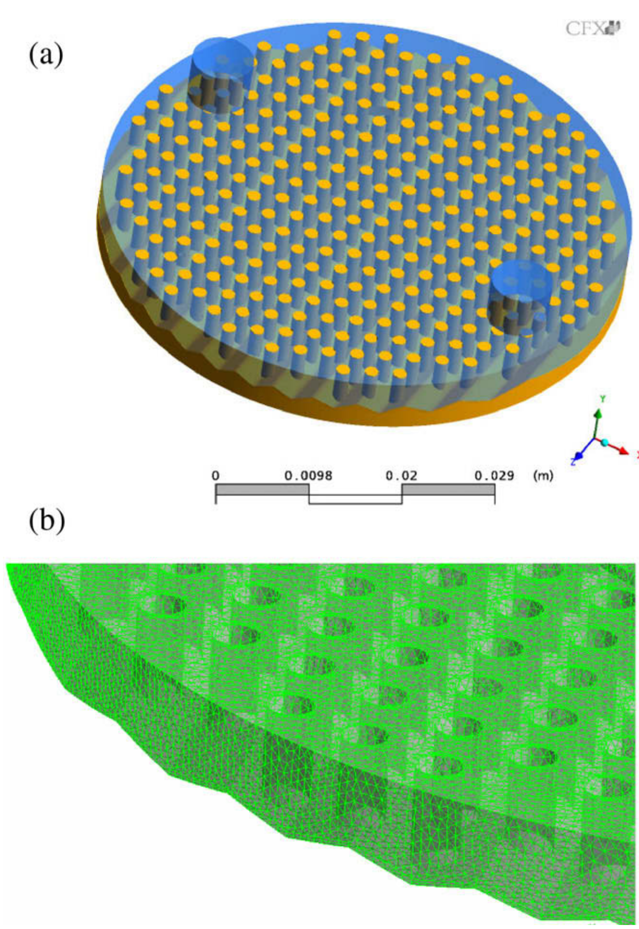

Fig. 3. (a) The computational domain of the cooling liquid flow path, and (b) detail of the grid.

5. Heat transfer augmentation using nanofluids

The heat removed from the hot water, Q_h, and the heat absorbed by the cooling liquid, Q_c are calculated by Eqs. (4) and (5) using the temperature and mass-flow rate data recorded. It is confirmed that they are practically equal, i.e., within the accuracy of the measuring technique, which is found to be less than 15%.

$$Q_c = Q = m_c c_{P,c}(T_{co} - T_{ci}) \tag{4}$$

$$Q_h = Q = m_h c_{P,h}(T_{hi} - T_{ho}) \tag{5}$$

In the above equations m is the mass-flow rate, c_P the heat capacity and T_i and T_o the inlet and outlet temperatures for the hot (h) and cold (c) stream, respectively. In Fig. 4 the heat transfer rate is presented versus the corresponding cooling liquid volumetric flow rate, V_c, for various hot water flow rates, V_h. It is observed that, when the CuO nanofluid is the cooling medium, the heat flow rate exhibits more than 10% increase compared to that of water. This heat transfer enhancement is also depicted in Fig. 5, where the total heat transfer coefficient, U, is plotted versus the volumetric flow rate for various hot water flow rates. The total heat transfer coefficient is calculated using Eq. (6) based on the experimental data and the real PHE surface area, A, which is equal to 6×10^{-3} m^2.

$$U = \frac{Q}{A \cdot F \cdot LMTD} \tag{6}$$

$$LMTD = \frac{(T_{ho} - T_{ci}) - (T_{hi} - T_{co})}{\ln\frac{(T_{ho} - T_{ci})}{(T_{hi} - T_{co})}} \tag{7}$$

The F factor depends on the temperature efficiency, P, the heat capacity ratio of the two streams, R, and the flow arrangement (Wang et al.,

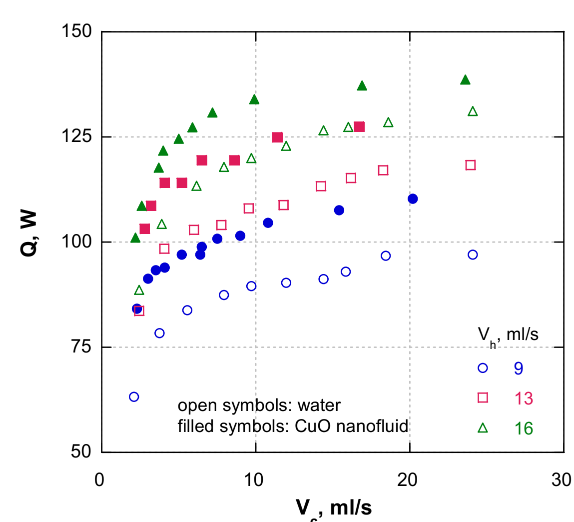

Fig. 4. Heat flow rate vs. cooling liquid flow rate for various hot water flow rates.

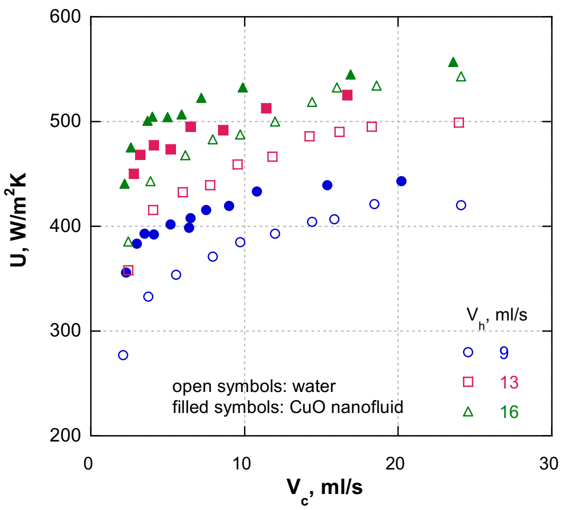

Fig. 5. Total heat transfer coefficient vs. cooling liquid flow rate for various hot water flow rates.

2007). In the miniature PHE the streams are not exactly in counter-flow, since part of the liquid flows around the plate circumference, as it will be shown later. Taking into account that in the present case the temperature efficiency and the heat capacity ratio are less than 0.2 and 2, respectively, it has been estimated that the F factor is greater than 0.97, even if the extreme case of cross-flow configuration is considered. Thus, for simplification F is taken equal to 1.

Available studies (e.g. Wen and Ding, 2004; Zeinali Heris et al., 2007), which were however performed in different geometrical arrangements, usually report that the enhancement is higher than in the present study. On the other hand, Nguyen et al. (2007b), who also conducted their experiments in a miniature PHE using a nanofluid with Al_2O_3 nanoparticles, observed almost 18% heat transfer enhancement (for 3.1% v/v suspension), a value close to the ones measured in the present study for the 4% CuO nanofluid. Fig. 5 reveals that, for a given hot water flow rate, the increase in the total heat transfer coefficient is more intense at lower cooling liquid flow rates. For example, for a hot water flow rate $V_h = 16$ ml/s, the increase in the total heat transfer coefficient is about 13% for $V_c = 6$ ml/s, but drops to 6% for $V_c = 15$ ml/s. This observation agrees with the experimental results by Chein and Chuang (2007), who examined the performance of a CuO–water nanofluid in a micro-channel heat sink. They report that at low flow rates the amount of energy absorbed by the nanofluids is greater than the corresponding amount for water, while at higher flow rates both the nanofluid and water remove almost the same amount of heat. This can be attributed to the fact that at high flow rates, where convection is the main heat transport mechanism, the contribution of the nanoparticles to the overall heat transfer rate turns out to be negligible, as also reported by Chein and Chuang (2007). A similar conclusion is drawn by Lee and Mudawar (2007) based on a theoretical analysis of heat transfer in a uniformly heated tube, where the nanofluid flows. According to the authors, for laminar flow the heat transfer coefficient is proportional to the fluid thermal conductivity, while for turbulent flow it depends mainly on the ratio of heat capacity over viscosity and in a smaller degree on the thermal conductivity of the fluid. Therefore, the effect of thermal conductivity becomes less pronounced, since, in the presence of nanoparticles, the aforementioned ratio decreases.

6. Numerical results

Initially, the effect of surface modulation on the heat transfer augmentation was numerically investigated by comparing the performance of the commercial miniature PHE to a similar notional heat exchanger with a plane surface (i.e., without modulation). Typical temperature distributions for both cases using water as the cooling medium are presented in Fig. 6 for a given heat duty.

Like typical PHEs (Kanaris et al., 2006), it is also obvious in this case that the surface modulation greatly promotes heat transfer. The mean plate temperature is found to be significantly lower (up to 10 °C) on the modulated plate than on the flat one. The results show that, as expected (Kanaris et al., 2006), the heat transfer rate increases up to 60% for the case of water compared to that of the flat plate PHE, which is more important than the enhancement invoked by the nanofluid. Regrettably, this heat transfer enhancement is accompanied by a significant increase (up to 2.5 times) of the corresponding friction losses. Therefore, the design of a PHE should be a compromise between heat transfer rate enhancement and pressure drop increase.

Another noteworthy observation concerns the type of flow inside the narrow passages of the PHE. As mentioned earlier, the modulated plate of the conduit comprises a significant number of pin-fins which increase the flow complexity and contribute to the heat transfer augmentation. Part of the fluid flows around the circumference of the plate unrestricted by the pin-fins, while the rest of the fluid follows the narrow passages between the pin-fins (Fig. 7a and c). It is observed that, as the flow rate increases, the fluid would rather follow the circumferential passage than the passages between the pin-fins. A closer look of the flow pattern (Fig. 7b and d) also reveals that for increased flow rates, the fluid avoids to flow around individual pin-fins (as seen in Fig. 7b), but rather circumvents them and follows the passages amid them and along the main axis of the flow (Fig. 7d). The latter can be attributed to the fact that, as Re increases, the length of the wake due to the cylindrical pin-fin becomes greater than the distance between the pin-fins (Bird et al., 2002), restraining the re-attachment of the flow. It is apparent that both cases of maldistribution have an impact on the heat transfer area utilization. To ameliorate this situation, the entry-point to the conduit might be placed away from the circumference, and/or the number of pin-fins might be increased to allow further heat transfer area utilization.

The results concerning the use of water and nanofluid as cooling liquids in the miniature PHE are in very good agreement with the experimental measurements (Figs. 8 and 9). From Fig. 8a it is obvious that the measured outlet temperatures of the cooling liquid are practically equal to the calculated ones. In Fig. 8b the same data are plotted in terms of heat flow rate and cooling liquid volumetric flow rate. In Fig. 9 the experimentally measured pressure drop of the cooling liquid, ΔP, in the heat exchanger conduit is compared to the respective values calculated by the CFD code. It is evident that the deviation between the experimental and predicted values is less than 5%, both for water and CuO nanofluid outlet temperatures and pressure drop, while in the case of heat flow rates it is less than 10%, proving that the computational method is reliable.

7. Evaluation of the use of nanofluids

In order to evaluate the performance of the nanofluid in the PHE and to compare it to that of water, the experimental data are plotted (Fig. 10a) in terms of heat load and pressure drop normalized with respect to the corresponding values of the base fluid versus the Reynolds number, Re, calculated using the physical properties of each liquid:

$$Re = \frac{uL\rho}{\mu} \tag{8}$$

where u is the liquid velocity and L the characteristic length, taken equal to the pin-fin height. It is observed that for a given Reynolds

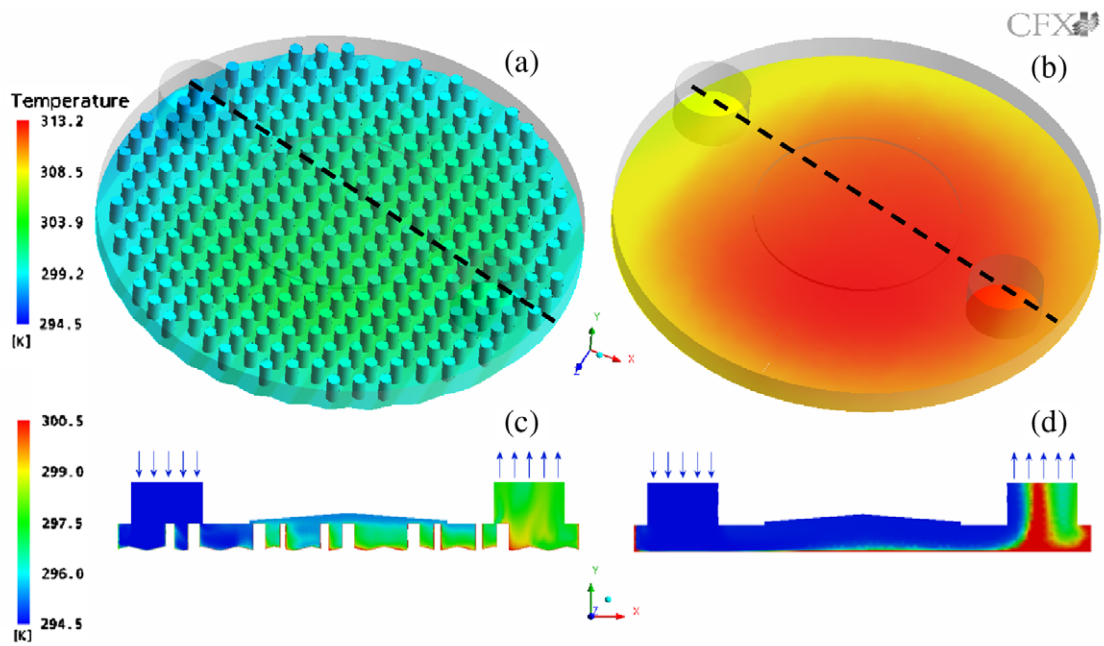

Fig. 6. Typical plate temperature distribution in a PHE with: (a) modulated, and (b) plane surface. Fluid temperature distribution at a flow cross-section for the case of: (c) modulated, and (d) plane surface.

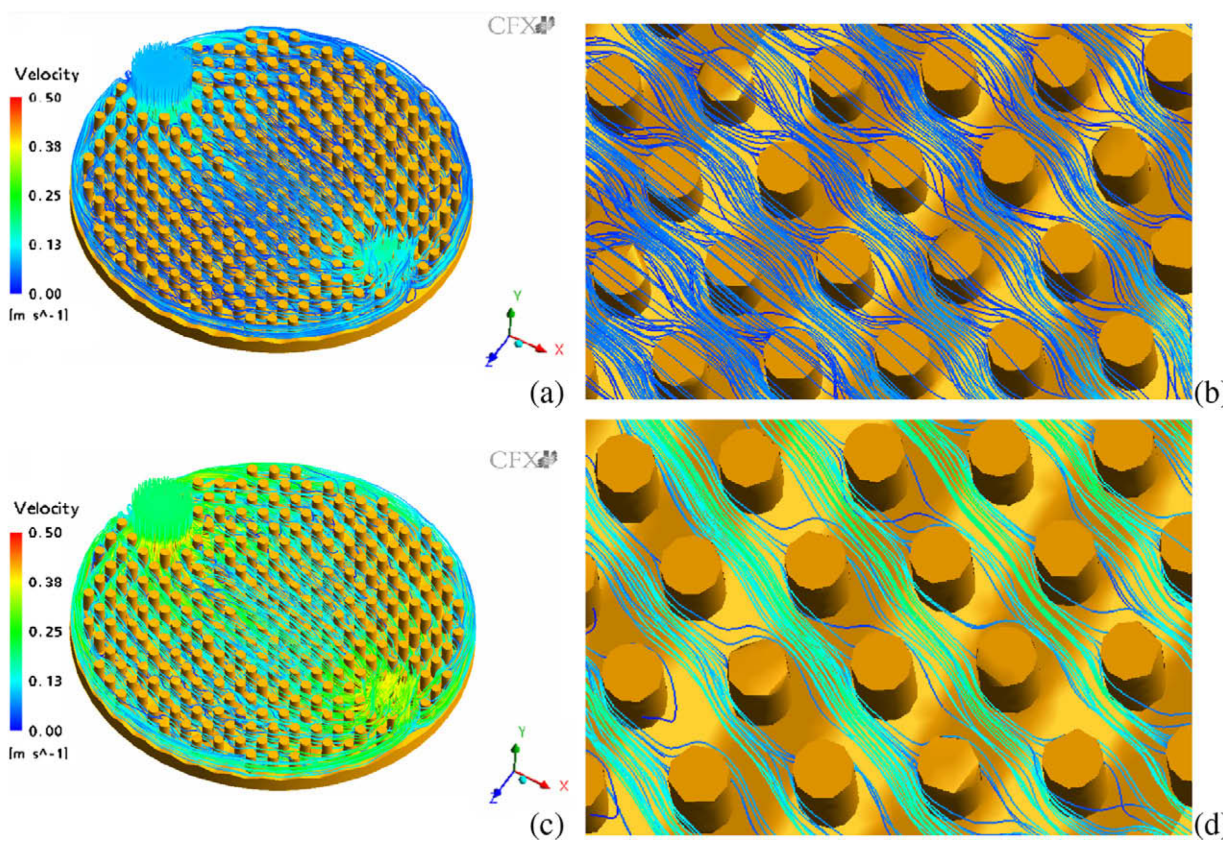

Fig. 7. (a and c) Typical streamlines in the miniature PHE, (b and d) a detailed view.

number (i.e., nanofluid flow rate higher than that of water, due to a higher kinematic viscosity), the normalized values are greater than 1, indicating that for the nanofluid both the heat transfer rate and the pressure drop are higher than the corresponding values for water. This type of presentation is usual for heat exchanging applications. However, for the kind of equipment considered in this study (i.e., CPU coolers), where the heat duty is predefined but at the same time the cooling medium volume and pumping power required are of crucial interest, the aforementioned presentation seems to be misleading. In the present case, when water is replaced

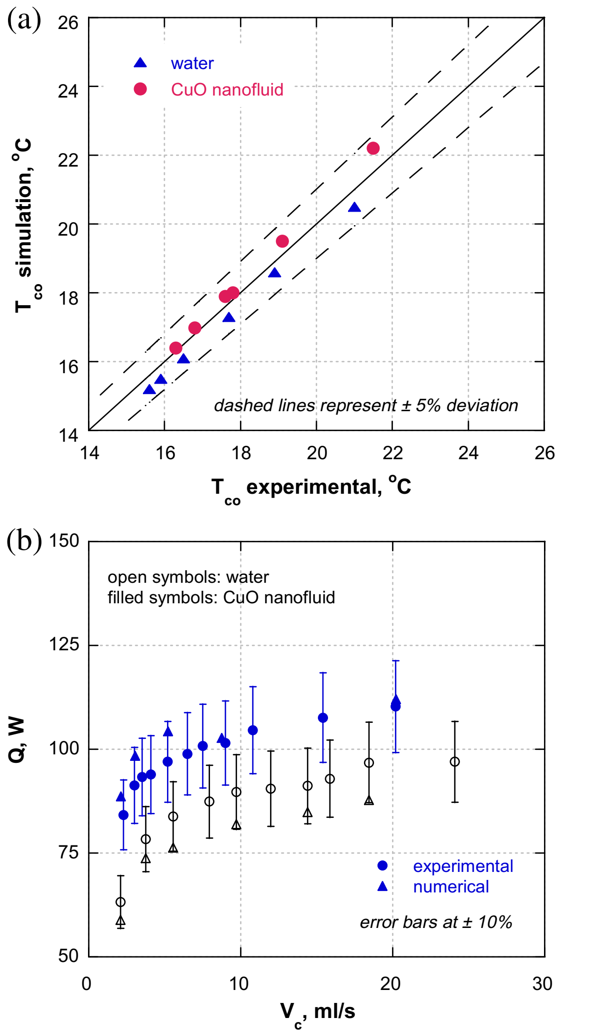

Fig. 8. Comparison of experimental and numerical results for: (a) cooling liquid outlet temperature, and (b) heat flow rate ($V_h = 9$ ml/s).

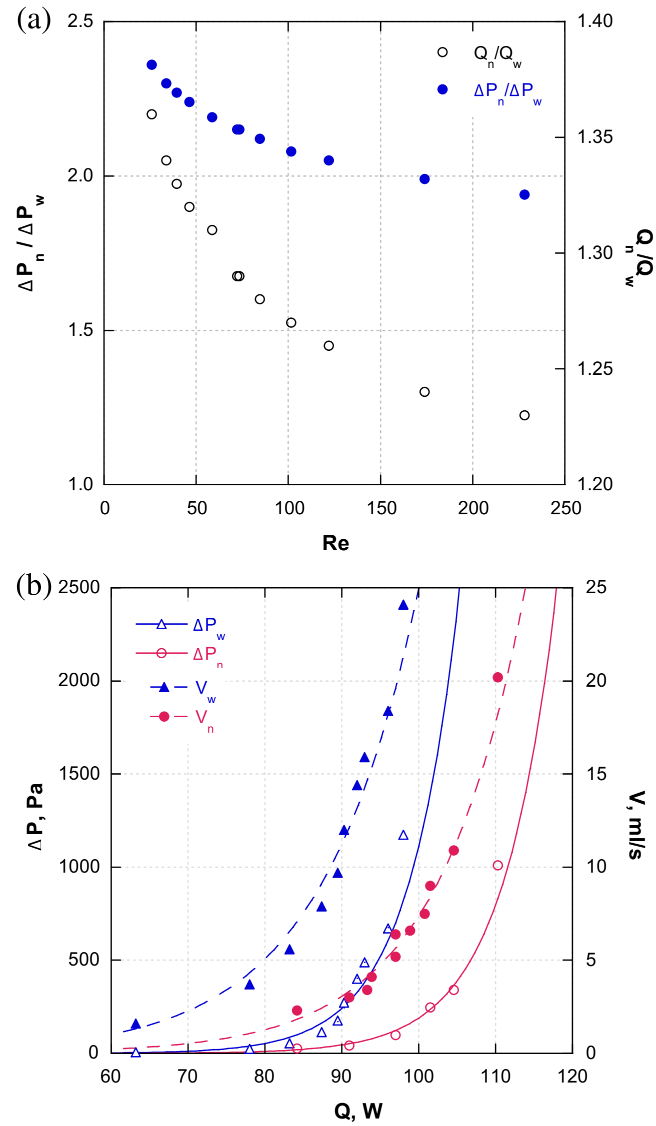

Fig. 10. (a) Normalized pressure drop and heat flow rate vs. Reynolds number for water and nanofluid, and (b) cooling liquid pressure drop and respective volumetric flow rate vs. heat flow rate.

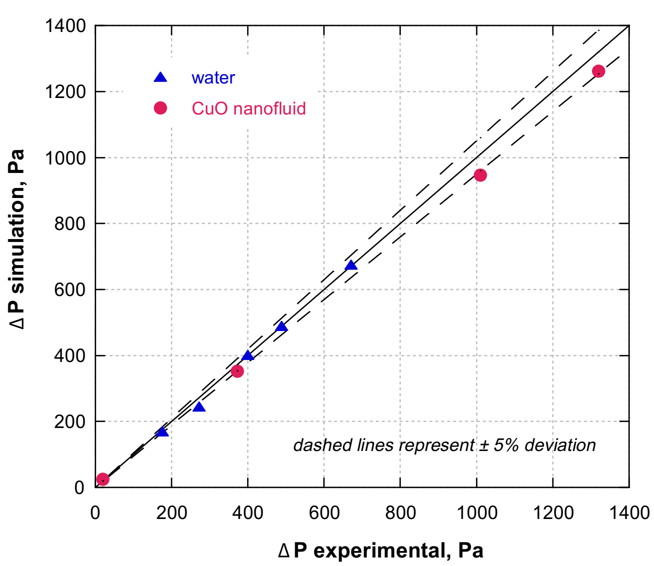

Fig. 9. Comparison of experimental and numerical results for cooling liquid pressure drop.

with the nanofluid, the aim is not to retain a constant Reynolds number, but to handle the same heat duty using less fluid and with the same or less pumping power. Therefore, a comparison in terms of the pressure drop inside the cooling liquid conduit for both fluids and the respective volumetric flow rates versus the heat transfer rate is considered essential (Fig. 10b). It is observed that for a given heat exchanger the use of the nanofluid leads to higher heat transfer rates, i.e., up to 115 W, while when water is used the heat transfer rate does not exceed 105 W. Moreover, for the same heat duty, e.g. 90 W, the water and nanofluid volumetric flow rates required are 11 and 3 ml/s, respectively, while the pressure drop is 240 and 45 Pa, respectively. This means that the nanofluid volumetric flow rate required in order to remove the specific heat load is almost **three** times lower than the respective value for water, while the pressure drop developed is about **five** times lower. It has already been reported that the viscosity of the nanofluid is higher compared to water. Therefore, as it is expected, for same volumetric flow rates, when the nanofluid is used, the measured pressure drop is higher than the respective value for water. However, when comparing the performance of the two cooling liquids in terms of a **given heat**

duty, the nanofluid pressure drop is lower due to its considerably lower flow rate.

In general and for all cases studied, it was found that the nanofluid flow rate required is up to 4 times lower (compared to water) while the respective pressure drop is up to 6 times lower. Consequently, not only can the nanofluid remove the same amount of energy by using a significantly lower flow rate, but it also requires less pumping power. This result is of great importance for designing heat transfer equipment, since it implies that in this kind of equipment, where the total volume is a main issue, the use of nanofluids contributes to the volume minimization, since, for a specific heat duty, less fluid is required compared to conventional cooling liquids. Furthermore, and for the same heat duty, the lower pressure drop developed when nanofluids are used, compensates for the increased friction losses caused by the surface modulation.

8. Conclusions

In the present study the consequences of employing a typical nanofluid (i.e., 4% v/v CuO) as working fluid in a miniature PHE were examined both experimentally and numerically. The thermophysical properties of the nanofluid were systematically measured and, as expected, it was found that the presence of the nanoparticles greatly affects the properties of the base fluid. The measurements reveal that, as also reported in the literature, the increase in the thermal conductivity is accompanied by a significant decrease in heat capacity and an increase in viscosity. However, the models and correlations available in the literature for the prediction of thermophysical properties do *not* always provide accurate results and thus they must be used with great caution.

The thermo-hydraulic behaviour of the PHE was also simulated using a CFD code. The results were in very good agreement with the experimental measurements and confirmed that the CFD is a useful and reliable tool for studying the PHE performance. However, when nanofluids are utilized, it is crucial to "feed" the code with accurate thermophysical data, which are not always readily available.

The heat transfer experiments confirmed that in a miniature *PHE* the substitution of water by a nanofluid generally enhances the heat transfer rate. More specifically:

- This enhancement is more pronounced at the lower cooling liquid flow rates tested. Yet, at higher flow rates, where convection is the main heat transport mechanism, the nanoparticle contribution to heat transfer seems to be less significant.
- The nanofluid volumetric flow rate required, for a given heat duty, is lower than that of water resulting in lower pressure drop and less pumping power.

In conclusion, the use of nanofluids seems to be a promising solution towards designing efficient heat exchanging systems, especially when the total volume of the equipment is a main issue. The only drawbacks so far for the extensive use of nanofluids are their high price and the possible instability of the suspension.

Acknowledgements

Financial support by the General Secretariat for Research and Technology and the European Union (*PENED 2003*) is greatly acknowledged. The authors would also like to thank Prof. M.J. Assael for his scientific advice and Dr. J. Tihon for his contribution to this work, as well as the Department technicians Mr. A. Lekkas, Mr. M. Bridakis and Mr. F. Lambropoulos for the technical support.

References

Assael, M.J., Chen, C.-F., Metaxa, I., Wakeham, W.A., 2004. Thermal conductivity of suspensions of carbon nanotubes in water. Int. J. Thermophys. 25, 971–985.
Bird, R.B., Stewart, W.E., Lightfoot, E.N., 2002. Transport Phenomena, second ed. John Wiley and Sons, Inc., New York.
CFX® Release 10.0 Manual. 2005. ANSYS Inc. International, Canonsburg.
Chein, R., Chuang, J., 2007. Experimental microchannel heat sink performance studies using nanofluids. Int. J. Therm. Sci. 46 (1), 57–66.
Ciofalo, M., Collins, M.W., Stasiek, J.A., 1998. In: Sundén, B., Faghri, M. (Eds.), Flow and Heat Transfer Predictions in Flow Passages of Air Preheaters: Assessment of Alternative Modeling Approaches. Computational Mechanics Publications, UK.
Das, S., Choi, S., Patel, H., 2006. Heat transfer in nanofluids – a review. Heat Transfer Eng. 27 (10), 3–19.
Das, S.K., Putra, N., Thiesen, P., Roetzel, W., 2003. Temperature dependence of thermal conductivity enhancement for nanofluids. J. Heat Transfer 125 (4), 567–574.
Hesselgraves, J.E., 2001. Compact Heat Exchangers: Selection, Design and Operation. Elsevier Science Ltd., Pergamon, Oxford, UK.
Hwang, K.S., Jang, S.P., Choi, S.U.S., 2009. Flow and convective heat transfer characteristics of water-based Al_2O_3 nanofluids in fully developed laminar flow regime. Int. J. Heat Mass Transfer 52 (1–2), 193–199.
Jung, J.-Y., Oh, H.-S., Kwak, H.-Y., 2009. Forced convective heat transfer of nanofluids in microchannels. Int. J. Heat Mass Transfer 52 (1–2), 466–472.
Kanaris, A.G., Mouza, A.A., Paras, S.V., 2006. Flow and heat transfer prediction in a corrugated plate heat exchanger using a CFD code. Chem. Eng. Technol. 29 (8), 923–930.
Lee, J., Mudawar, I., 2007. Assessment of the effectiveness of nanofluids for single-phase and two-phase heat transfer in micro-channels. Int. J. Heat Mass Transfer 50 (3–4), 452–463.
Lee, S., Choi, S.U.S., Li, S., Eastman, J.A., 1999. Measuring thermal conductivity of fluids containing oxide nanoparticles. Trans. ASME J. Heat Transfer 121 (2), 280–289.
Leitner, J., Sedmidubsky, D., Dousova, B., Strejc, A., Nevriva, M., 2000. Heat capacity of CuO in the temperature range of 298.15–1300 K. Thermochim. Acta 348 (1–2), 49–51.
Maiga, S.E.B., Palm, S.J., Nguyen, C.T., Roy, G., Galanis, N., 2005. Heat transfer enhancement by using nanofluids in forced convection flows. Int. J. Heat Fluid Flow 26, 530–546.
Mansour, R.B., Galanis, N., Nguyen, C.T., 2007. Effect of uncertainties in physical properties on forced convection heat transfer with nanofluids. Appl. Therm. Eng. 27 (1), 240–249.
Menter, F., Esch, T., 2001. Elements of industrial heat transfer predictions. In: 16th Brazilian Congress of Mechanical Engineering (COBEM), Uberlandia, Brazil, 26–30 November.
Nguyen, C.T., Desgranges, F., Roy, G., Galanis, N., Mare, T., Boucher, S., Angue Mintsa, H., 2007a. Temperature and particle-size dependent viscosity data for water-based nanofluids – Hysteresis phenomenon. Int. J. Heat Fluid Flow 28 (6), 1492–1506.
Nguyen, C.T., Roy, G., Gauthier, C., Galanis, N., 2007b. Heat transfer enhancement using Al_2O_3–water nanofluid for an electronic liquid-cooling system. Appl. Therm. Eng. 27 (8–9), 1501–1506.
Pak, B.C., Cho, Y.I., 1998. Hydrodynamic and heat transfer study of dispersed fluids with submicron metallic oxide particles. Exp. Heat Transfer 11 (2), 151–170.
Roy, G., Nguyen, C.T., Lajoie, P.-R., 2004. Numerical investigation of laminar flow and heat transfer in a radial flow cooling system with the use of nanofluids. Superlattice Microstruct. 35, 497–511.
Trisaksri, V., Wongwises, S., 2007. Critical review of heat transfer characteristics of nanofluids. Renew. Sust. Energy Rev. 11 (3), 512–523.
Tsai, T.-H., Chein, R., 2007. Performance analysis of nanofluid-cooled microchannel heat sinks. Int. J. Heat Fluid Flow 28 (5), 1013–1026.
Wang, L., Sunden, B., Manglik, R.M., 2007. Plate Heat Exchangers. WIT Press, Southampton, Boston.
Wang, X.-Q., Mujumdar, A.S., 2007. Heat transfer characteristics of nanofluids: a review. Int. J. Therm. Sci. 46 (1), 1–19.
Wen, D., Ding, Y., 2004. Experimental investigation into convective heat transfer of nanofluids at the entrance region under laminar flow conditions. Int. J. Heat Mass Transfer 47, 5181–5188.
Wilcox, D., 1988. Reassessment of the scale-determining equation. AIAA J. 26 (11), 1299–1310.
Williams, W., Buongiorno, J., Hu, L.-W., 2008. Experimental investigation of turbulent convective heat transfer and pressure loss of alumina/water and zirconia/water nanoparticle colloids (nanofluids) in horizontal tubes. J. Heat Transfer 130 (4), 042412–042417.
Xuan, Y., Li, Q., 2003. Investigation on convective heat transfer and flow features of nanofluids. J. Heat Transfer 125, 151–155.
Xuan, Y., Roetzel, W., 2000. Conceptions for heat transfer correlation of nanofluids. Int. J. Heat Mass Transfer 43, 3701–3707.
Zeinali Heris, S., Nasr Esfahany, M., Etemad, S.G., 2007. Experimental investigation of convective heat transfer of Al_2O_3/water nanofluid in circular tube. Int. J. Heat Fluid Flow 28 (2), 203–210.
Zhou, S.Q., Ni, R., 2008. Measurement of the specific heat capacity of water-based Al_2O_3 nanofluid. Appl. Phys. Lett. 92 (9).